

Scratch Assay Assessment Benchmark

Michael Linortner¹[0000-0002-6706-4450] and Andreas Uhl¹[0000-0002-5921-8755]

Department of Artificial Intelligence and Human Interfaces, University of Salzburg,
Jakob-Haring-Str. 2, 5020 Salzburg, AT
{mlinortner, uhl}@cs.sbg.ac.at

Abstract. Scratch assay evaluation is a widely used and standardized method for investigating collective cell migration and wound healing processes. Modern laboratory technology offers the possibility of high-resolution digital image acquisition leading to the use of computer vision methods for the analysis of scratch assays. Benchmarking is necessary to measure the performance of newly developed analytical tools. Publicly available data sets and software tools are needed to ensure objective and reproducible testing. This work presents a new dataset consisting of high-resolution raw images obtained with an industrial plate reader together with ground truth data manually annotated by experts to overcome the sparse availability of annotated scratch assay images. The advantage of this dataset over other publicly available datasets is its much higher resolution (up to 10 times). It also covers the entire cell layer in a well, allowing the entire wound area to be examined rather than just the central region. In addition to the dataset, a software tool will be published containing two algorithms developed to measure wound healing using the presented data. Their performance will be compared with other publicly available tools.

Keywords: Scratch assay · benchmark · wound healing assessment · scratch assay database.

1 Introduction

Wound healing assays, also known as scratch assays, are standardized procedures for studying cell migration processes under laboratory conditions. These assays are confluent monolayers of a specific cell type grown in a container called a well. By mimicking a wound by inflicting a scratch to the cell monolayer, collective cell migration processes can be studied in vitro in a two-dimensional space: cells start to move and grow into the cell-free area of the scratch until a confluent cell layer is eventually reestablished. This helps to model and understand wound healing processes and provides a standardized, cost-efficient technique. To measure these migration processes, images of the assays are acquired at regular time intervals, which can then be analyzed either by experts or automatically using computer vision tools [11, 9, 6]. The percentage of wound area reduction or closure can be used as a standard measure of wound healing. It is calculated as follows [6, 15]:

$$\text{wound closure in \%} = \left[\frac{A_{t=0} - A_{t=\Delta t}}{A_{t=0}} \right] \times 100, \quad (1)$$

with $A_{t=0}$ referring to the initial wound area, and $A_{t=\Delta t}$ representing the wound area measured after a time laps of Δt . The wound area can be measured by counting these pixels which have been classified as a wound area (cell-free background). The process of dividing image pixels into cell and non-cell classes is called segmentation.

This section provides a brief overview of several implementations of algorithms related to collective cell migration processes using computer vision tools. A software tool called TScratch is presented by Gebaek et al. in [3], which applies an edge detection algorithm based on the discrete curvelet transform. The computed curvelet coefficients represent the amount of detail in the image areas. Those regions with a lot of detail are classified as cell areas. A tool called MultiCellSeg has been presented by Zaritsky et al. in [17]. The algorithm divides the image into small patches and computes texture-based features, like smoothness and gradient histograms, gray level values, ratio of local and global intensity values. Pre-trained support vector machines (SVMs) are separately applied to these features to classify the patches as cell and background areas. In a second cascade, another SVM is applied to discard misclassified background areas. In the final step, a graph-cut based segmentation algorithm refines the previous classification to produce the final segmentation output. Glass et al. [4] use topology-preserving level sets to identify the boundary between the confluent cell layer and the wound area. An entropy-filter is applied for preprocessing and an entropy-based heuristic is utilized to remove falsely detected wound area parts, which was replaced by a support vector machine (SVM) approach in a follow-up study [5]. Moeller et al. [13] use active contours (snakes) to detect the boundaries between wound and cell areas. Topman et al. [16] compute the pixel standard deviation and use a histogram-based threshold, while Cortesi et al. [2] apply local entropy filter with Otsu’s method for threshold finding. Suarez et al. [15] utilize a local variance filter followed by local thresholding. Sinitca et al. [14] present a tool called BCAnalyzer, which computes a local edge density image on the output of the Canny edge detection algorithm. The final segmentation is obtained using a user-defined or automatically determined threshold value. A convolutional neural network (CNN) is presented by Javer et al. [8]. The CNN identifies cells and labels these pixels. In the post-processing step, morphological operations are applied to the labeled output and finally all unlabeled pixels are identified as wound area. Table 1 gives an overview of the publicly available implementations of the proposed techniques described above.

In addition to the software tools, there are a number of small databases publicly available, containing scratch assay image series. Those are listed in table 2. BBBC019 [12] provides a bundle of datasets including but not limited to scratch assays¹. The HuTu80 database [14] is available with the BCAnalyzer software tool and can be retrieved from gitlab². All these datasets contain one to several time series of cell migration processes with only a few images per sequence. All images show the center region of a scratch assay and mainly contain

¹ <https://bbbc.broadinstitute.org/BBBC019>

² <https://gitlab.com/digiratory/biomedimaging/bcanalyzer>

Table 1: List of publicly available software implementations for scratch assay assessments.

Tool	SW-Language	Algorithm
TScratch [3]	MATLAB	Edge-detection based on discrete curvelet transform
MiToBo SAA [4, 5]	ImageJ plugin	Entropy filter + level sets + SVM
CellProfiler [1, 10]	Python	Intensity based
Cell Invasiv-o-Meter [2]	MATLAB	Local entropy
WHST [15]	ImageJ plugin	Texture filter based on local variance
BCAnalyzer [14]	Python	Local edge density + threshold
MultiCellSeg [17]	MATLAB	Several texture-based features + SVM

images of the earlier migration process where no defragmentation of the wound area has yet taken place.

The contribution of this research is a new publicly available dataset (PLUS-ScratchAssay-DB)³ containing scratch assay images depicting a cell migration process together with ground truth masks, annotated by experts. The advantages over existing datasets are: the high resolution (up to 10 times higher) of the raw images, the image frame covering the entire cell layer of a well and the fine resolution of the cell migration process with 34 images in a single sequence. Together with the dataset, the PLUS Scratch Assay Analyzer software tool is made publicly available⁴. The tool contains two new algorithms, which have been developed in the course of a previous work [7]. The performance of both algorithms is evaluated on the data, presented and compared with the results achieved by the publicly available tools.

The database is presented in detail in section 2 of this manuscript. Section 3 describes the design of two experiments and the measures used to evaluate the performance of the PLUS Scratch Assay Analyzer software tool and the publicly available algorithms on the new dataset. The results of these experiments are presented in section 4. This is followed by a discussion of the challenges of the cell migration process segmentation task in section 5. The findings of this study are summarized in the conclusion section.

2 Provided Database

In this manuscript, a new database consisting of one time series of scratch assays is presented. Its characteristics are summarized in table 3.

The database consists of 34 bright field images representing one single time series observing the cell migration process of one scratch assay. The images have been acquired with an industrial plate reader. Figure 1a shows the first image of the sequence. Together with the bright field images, a ground truth is provided which has been manually annotated by experts. In comparison to the already

³ <https://wavelab.at/sources/Linortner24a/>

⁴ <https://wavelab.at/sources/Linortner24a/>

Table 2: Publicly available data sets containing scratch assay time series.

Database	Data set	No. Img	Resolution	Format	No. Seq.	No. Img/Seq.
BBBC019 [12]:						
	TScratch	24	1384 × 1028	jpg	12	2
	Melanoma	20	1280 × 1024	jpg/tif	10	2
	Init	22	1024 × 1024	tif	2	11/11
	SN15	54	1024 × 1024	tif	26	1-3
	HEK293	12	512 × 512	tif	12	1
	MDCK	14	1024 × 1024	tif	8	1-3
HuTu80 [14]:						
	HuTu80	180	1388 × 1040	png	6	5/6/9/5/10/10

Table 3: The PLUS-ScratchAssay-DB database.

Database	No. Images	Resolution	Format	No. Seq.
PLUS-ScratchAssay-DB	34	9824 × 10260	tiff	1

publicly available databases from table 2, this new database offers the following advantages: Although containing only one time series of a single cell monolayer, this sequence contains 34 images and depicts the course of cell migration from the initial scratch to the end where the cells build again a confluent layer at a fine granular time resolution. The images cover the entire well and therefore, offer the possibility to investigate the migration process over the entire cell layer and wound area. A third advantage offer the data format: the high resolution images are stored in a raw data format directly provided by the well plate reader. As a consequence, additional topics can be investigated, like the impact of compression rate on the accuracy of cell segmentation algorithms.

3 Experimental set-up

In the following, two experiments are presented: the first one compares the performance of the publicly available software tools listed in table 1 in comparison with two algorithms developed by us [7]. All these software tools from table 1 are not able to handle images where the well border is present. They need center cropped images only showing cell/wound area. Therefore, a second experiment is conducted to provide a benchmark for the wound area segmentation exploiting the whole scratch assay area of a well, using solely our algorithms.

3.1 Experiment A: performance comparison of the publicly available tools

The publicly available software tools listed in table 1 have been analyzed and tested on the database presented in this manuscript. To achieve reasonable performance results, a maximum of 8 working hours per tool was scheduled for tuning the parameters.

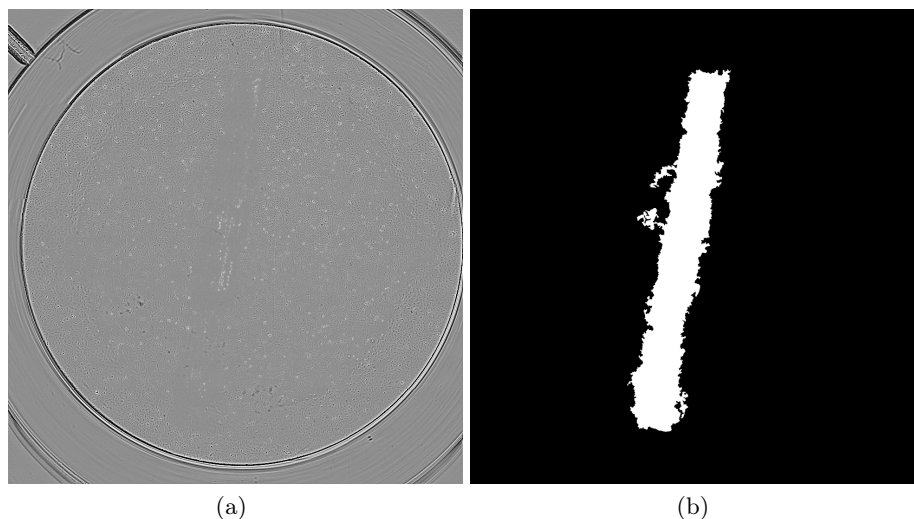


Fig. 1: (a) shows the first image of the PLUS-ScratchAssay-DB, (b) the ground truth segmentation for that image.

Experiment A is conducted on center cropped images of size 4800 x 4500 pixels of the original data. This is necessary as all tools from table 1 are not able to handle the well border present in the PLUS-ScratchAssay-DB images.

Three tools have been excluded from the experiment due to reasons explained in the following. The Cell Invasiv-o-Meter [2], a MATLAB tool with graphical user interface (GUI), needed some adaption that it was even able to run it on a more recent MATLAB version resulting in incorrect output, conceivably due to version incompatibility. Further, it did not provide any parameter to tune the behavior of the algorithm to produce a meaningful output.

The CellProfiler [1, 10] is an application with GUI for detecting cells, cell colonies or tumor areas and includes a tool for scratch assay evaluation. The wound/cell area detection is mainly based on utilizing the pixels intensity levels. It is not applicable on our data: It detects darker spots which consist of artifacts (dead cells, dirt) and the central regions of cells. The remaining area is considered as background. It detects background over the whole cell area, consisting of wound regions, the small interspace between cell in the confluent area but also miss classifies the outer regions of single cells as background. Hence, it is not able to recognize the boundary between cell and wound area as can be seen in figure 2a and 2b. It was not possible to tune the parameters to detect wound area and ignore the small interspaces in the cell region. Using a sample image from [17], which has no uniform background illumination, it can be observed that the algorithm segments the bright area from the darker area. It ignores any textural structure present in the cell area or absent in the wound area, see figure 2c and 2d.

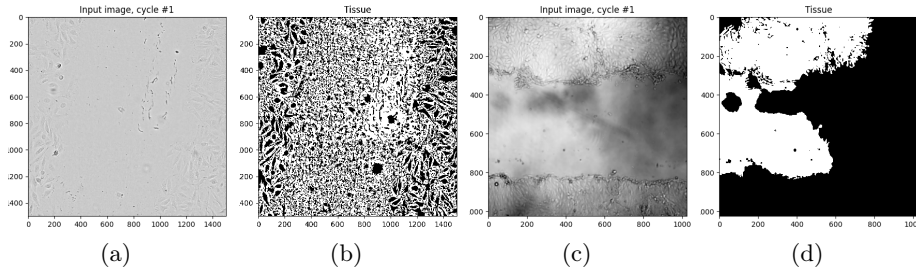


Fig. 2: Segmentation results produced by the CellProfiler software: (a), (b) show a detail from an image of PLUS-ScratchAssay-DB and (c), (d) the segmentation on a data sample from [17].

The MultiCellSeg software from [17] solely utilizes pre-trained SVMs, trained on differential interference contrast (DIC) images like in figure 2c and does not provide any parameters to tune. It does not detect any wound pixels in our data at all. It would be necessary to train their SVMs on our data. The download link provided in [17] is not working anymore, but using the wayback machine (<https://wayback-api.archive.org>) it was possible to retrieve the software package.

The following tools have been utilized successfully in the experiment: TScratch [3] is a MATLAB tool with GUI to process scratch assay images. There are several parameters which could be configured before analyzing the data. After processing the images the segmentation result for each image is displayed and the segmentation threshold can be adjusted manually either globally for all images or individually for each single image. The effect on the segmentation result can be immediately seen on the screen, which helps to find a suitable threshold value for a reasonable wound area segmentation. In the experiment we only used a global threshold value for all images and skipped individual adjustment, which follows the same procedure applied on the other tools.

The MiToBo Scratch Assay Analyzer (MiToBo SSA)[4, 5] is a plugin for Fiji/ImageJ. The tool provides a GUI for loading a sequence of images and adjusting parameter values.

The Wound Healing Size Tool (WHST) [15] is another plugin for ImageJ designed to detect cell-free areas in scratch assay images. In the final processing step, it selects the cell-free area with the largest size as the segmentation result assuming this would be the wound area. This could lead to inaccurate results if the wound area starts to defragment in the later stages of the cell migration process or some region outside the cell-layer happens to be the largest cell-free area, e.g. the well border in the PLUS-ScratchAssay-DB images.

The fourth publicly available tool applied within this experiment is the BC-Analyzer [14]. It is a python implementation offering a GUI for analyzing scratch assay images. The software needed an adaptation to be able to load images provided in the TIFF format.

None of the four tools presented above offer a command line interface or a possibility to fully automatically evaluate scratch assays without user interaction being needed. Hence, it would be fair to say that it is somewhat cumbersome to adjust all the algorithms' parameters to find a configuration that ultimately produces a segmentation output that is reasonable good and accurate in comparison to the provided ground truth. The BCAnalyzer software has been modified to accommodate the loading of images in TIFF format. Additionally, a command line interface has been developed to facilitate the processing of a sequence of scratch assay images in conjunction with a configuration file that specifies the values for the algorithm's parameters. The BCAnalyzer tool is a well structured python program which allowed an easy modifications of the source code. These adaptations have already been implemented in the course of a previous work [7].

PLUS Scratch Assay Analyzer: Log Gradients and Entropy Filter segmentation algorithm Next to the aforementioned tools, a new software implementation is applied on the dataset: the PLUS Scratch Assay Analyzer. It is implemented in MATLAB and accessible from the command line, making it suitable for automatic image processing, either to operate on a large amount of data or to conduct an extensive parameter value search to optimize its performance on the given data. The analyzer tool provides two algorithms: the Log Gradients (LG) and the Entropy Filter (EF) segmentation. Both algorithms have been developed in the course of a previous work [7]. In short, the EF algorithm uses a local entropy filter in the first step followed by several morphological operations in order to detect a continuous wound-cell boundary. The final step uses Otsu's method to find an adaptive threshold. The LG algorithm calculates local gradients and produces a Laplacian of Gaussian (LoG) map histogram, which is used to classify cell and cell-free areas. This is followed by a refinement step to remove small isolated components that are considered as noise. See [7] for a detailed descriptions of these methods.

3.2 Experiment B: Benchmark on PLUS-ScratchAssay-DB

In the experiment described in the previous sections, only center cropped images of the PLUS-ScratchAssay-DB were used, because this is required by the publicly available software tools examined. In section 2 it was mentioned that an advantage of the presented database is that the entire cell area of a well, and therefore the entire scratch, can be analyzed. Consequently, a second experiment is conducted on the the PLUS-ScratchAssay-DB images, using the entire image section. The performance of the LG and EF algorithms have been evaluated and serve as a initial benchmark on the PLUS-ScratchAssay-DB.

3.3 Measures

The performance of the algorithms is measured by comparing the size of the segmented wound are to the ground truth segmentation. To analyze the accuracy of

the segmentation the intersection over union (IoU) is computed, which measures how precise the overlay between the segmentation output and the ground truth segmentation is. It measures the ratio of the overlapping area to the total area covered by the union of the two segmentations. The IoU is computed as follows:

$$IoU = \frac{|S \cap G|}{|S \cup G|}, \quad (2)$$

where S is the segmentation output of the algorithm and G is the ground truth segmentation. Figure 3 depicts the overlay of the segmentation output and the ground truth segmentation, visualizing the concept of IoU.

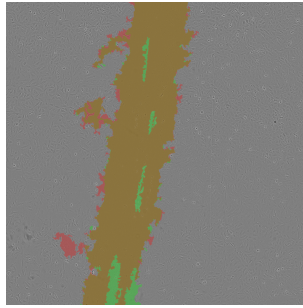


Fig. 3: Intersection over union (IoU) example: Green is the ground truth segmentation G , red is the segmentation output S of the LG-algorithm and the brownish area shows the overlapping segmentation result.

4 Results

This section presents the results of the two experiments described in the experimental set-up section.

4.1 Performance comparison of the publicly available tools

Figure 4 shows the results of the wound area segmentation task of the presented algorithms and the publicly available tools in comparison to the ground truth. The segmented area is shown as a fraction of the total image area. It can be observed that the segmentation results of the different tools diverge considerably from each other and from the ground truth, especially the MiToBo Scratch Assay Analyzer and the TScratch tool. The LG, BCAnalyzer and WHST tools produce a result that is closer to the ground truth, notable between 5 and 15 in the time sequence. In the later stages of the wound healing, the wound areas become smaller and start to defragment, making it quite a challenge for the algorithms to identify the correct parts in the image. In the case of the WHST tool, the

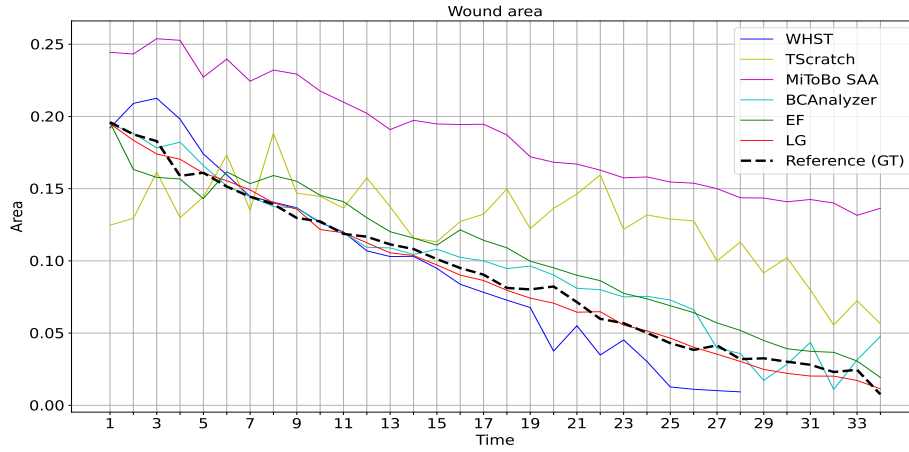


Fig. 4: Results of experiment A: The size of the segmented wound area in comparison to the ground truth (GT). The area of the segmented wound is given relative to the total image area.

detected wound area is consistently smaller than the ground truth. The reason for this is, that the tool only considers a single blob with the largest size of all detected cell-free areas as the wound area, which is no longer true when the wound area is divided into separate parts during the cell migration process. The graph of the WHST tool stops at sequence number 28 because an unknown error occurred while processing the following images. A possible explanation for the lower performance of the MiToBo SSA and the TScratch tool may be that they were developed on a different dataset and the algorithms have their difficulties with the divergent appearance of the cell layer in the database provided in this experiment. In addition, further fine-tuning of the parameters may improve the performance of these algorithms.

4.2 Benchmark on the PLUS-ScratchAssay-DB

Figure 5 shows the segmentation results of experiment B obtained by the two presented segmentation algorithms Entropy Filter (EF) and Log Gradients (LG) on the original data of the PLUS-ScratchAssay-DB. In figure 6, the accuracy of the wound area segmentation is depicted by measuring the intersection over union. It shows that as cell migration (wound healing) progresses, the IoU measure decreases. In the later stages of the sequence the wound area starts to defragment and become smaller, making it quite challenging to detect these areas and distinguish them from the natural spaces between the cells in the surrounding confluent layer. These difficulties will be examined in more detail in the following discussion.

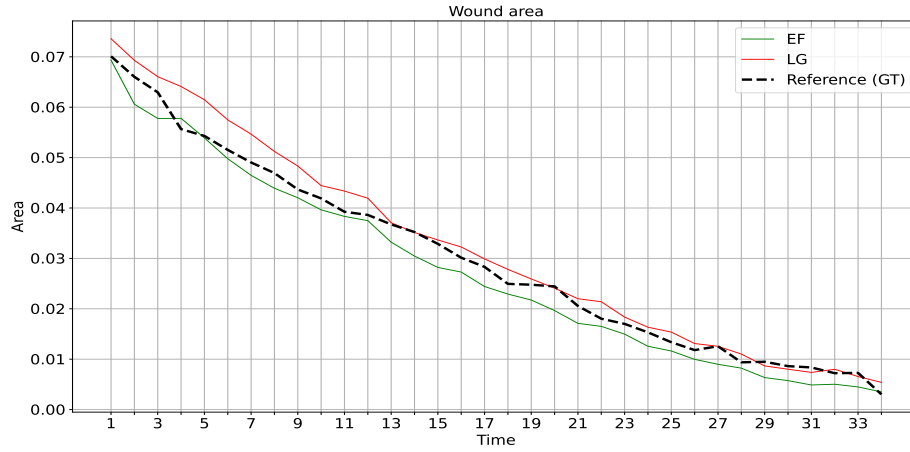


Fig. 5: Results of experiment B: The size of the segmented wound area by the LG and EF algorithm in comparison to the ground truth (GT). The area of the segmented wound is given relative to the total image area.

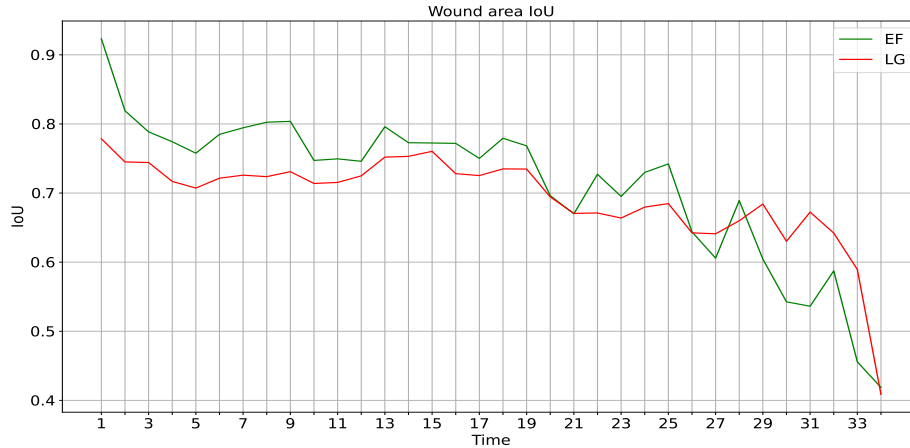


Fig. 6: Results of experiment B: The intersection over union (IoU) of the segmented wound area and the ground truth.

5 Discussion on challenges

Summarizing, the results show that the two developed algorithms (LG and EF) can compete with existing wound area segmentation tools and even outperform them for the given data. The experiments also reveal that in the later stages of the cell migration process, acquired in the later images of the data sequence, the performance drops, as can be observed from the IoU outcomes in figure 6. In the later stages of the sequence, as the wound area becomes smaller and begins to

defragment and if the adjacent cell area is less confluent, it becomes more difficult to select the correct wound areas and the IoU begins to decrease rapidly. Some additional factors discussed below will also play a role. Overall, the results show that there is definitely potential to increase the accuracy of the segmentation output and therefore this topic deserves further attention. The work on this study revealed some challenging tasks for the wound area segmentation process, which are discussed below.

Initial scratch detection During the wound area detection process, the algorithm may detect cell-free areas outside the wound area. As a result, these erroneously detected regions are included in the resulting wound area. This phenomenon is frequently observed to result from a reduction in the degree of confluence of the cell layer during the migratory process, or because of artefacts or changes in image quality during the imaging process. Especially when processing the well images as a whole, at the region towards the well border the image quality/contrast/sharpness can drop or the cell layer appears less confluent, which can be observed in figure 7a. In the first image of a sequence, the wound area is clearly the largest contiguous cell-free region and it is therefore easier to remove erroneously detected regions, which tend to be smaller in size. In contrast, in the later stages of the migration process, the wound area shrinks and it is difficult to remove false positives as they are not necessarily different in size. Furthermore, it can occur that small false positive areas adjacent to the wound area are connected to the wound area by thin paths between cells caused by noise or image quality issues etc. To avoid these issues, a profound initial scratch detection can help: In the first image of a sequence, the wound area, or more precisely the boundary of the wound area, appears more clearly than in the later stage of the cell migration process. It is therefore easier to detect the scratch area in the first image. Once the wound has been successfully detected, it can be masked as a region of interest. The EF algorithm already incorporates this approach. It creates a mask that is the detected wound area in the first image with an added margin. Only this region of interest is processed in subsequent images. However, it is based on the premise that it can detect the wound area as a contiguous area with the largest size of all cell-free areas found. As EF works on a local scale, the process could be improved by examining the initial image in a coarser view by scaling down the image, applying a texture filter and attempting to detect the wound area using, for example, a Difference of Gaussian operation. Obviously, this will not give an exact result but it serves to detect the region of interest. Figure 7 illustrates this idea. In figure 7a it can be seen that the cell layer appears more confluent towards the center than towards the edge of the well.

Problem of tracking cell fragments In the initial wound area, it is assumed that the whole area is free of cells. If there are some cells left, they are just remnants of the scratch generation and are not part of the cell migration process. Therefore, these areas can be filtered out to obtain a continuous wound area. In

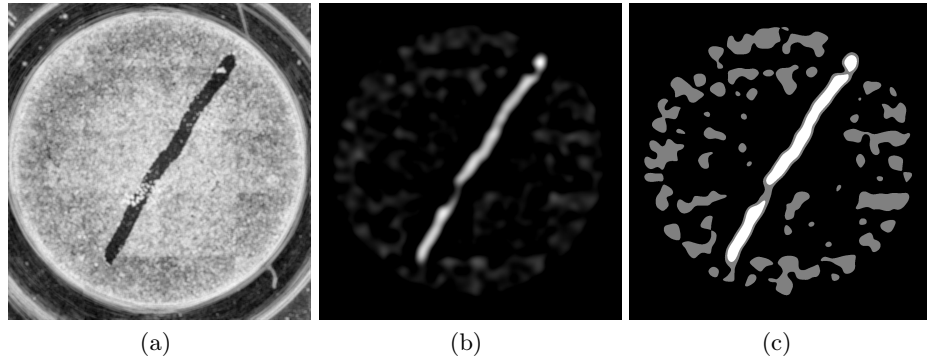


Fig. 7: Steps for scratch detection: (a) filter response (entropy filter) on a down scaled input image, (b) Difference of Gaussian, (c) segmentation result utilizing a multi-threshold method.

the first image of a sequence, this is a fairly straightforward process. However, in the later stages of the cell migration, some cells may migrate into the wound area and form small islands. The question now is which of the small islands of cells in the wound area should be removed and which should be retained? At what stage in the sequence do we stop removing small islands of cells as artefacts or cell remnants of the initial scratching process?

Dirt in wound area A closely related topic is the presence of dirt in the wound area. Both algorithms (EF and LG) try to detect uniform background area. Therefore, non-uniform background area can not be distinguished from cell-area. EF detects areas of high entropy, while LG detects areas with high and varying gradients, which is true for both cells and dirt. Of course, the same questions arise as in the paragraph above: At what point do we stop removing these areas because they are already migrated cell clusters?

Difficulties in detecting the boundary of the wound area In general, it is a challenging task to accurately identify the boundary of the wound area. This is especially true in images where cell migration is in progress. In the initial image, the scratch boundary is quite well defined, but during the cell migration this border starts to become more fragmented, many bays and islands appear, and also the transition between cells and background is often vague, as in figure 8d.

Summarizing the difficulties and future work As discussed above, due to the nature of the smooth transition between cell area and wound area/background and the fine defragmentation of this boundary it is quite difficult for the methods to accurately detect this boundary. The filter response of the EF algorithm

enhances those areas with more texture information: the cell area, but also noisy regions. Slight variations in the amplitude of the response ultimately determine whether a pixel is classified as background or cell area. Local variations in intensity values also make it difficult to use a threshold. Even methods for automatically finding local thresholds struggle. Often these methods attempt to balance the ratio of foreground to background. However, this ratio varies greatly across a scratch assay image. It turned out that the best methods were auto-threshold methods applied to the whole image. After the binarization process, the area around the boundary is very cluttered. To obtain a continuous boundary, morphological post-processing is required to remove noise and connect defragmented boundary regions. But after binarization, all information is lost, whether a pixel is noise or could be part of a cell. Therefore, it is of interest to apply deep learning methods to the wound segmentation task. It could be considered to introduce a multi-class classification: for example, an approach where background (figure 8a), artefacts/dead cells/dirt (figure 8b) and cells (figure 8c) can be distinguished. This would help in a morphological post-processing to remove noise more accurately. Another approach could be the direct detection of the cell-wound boundary as shown in figure 8d.

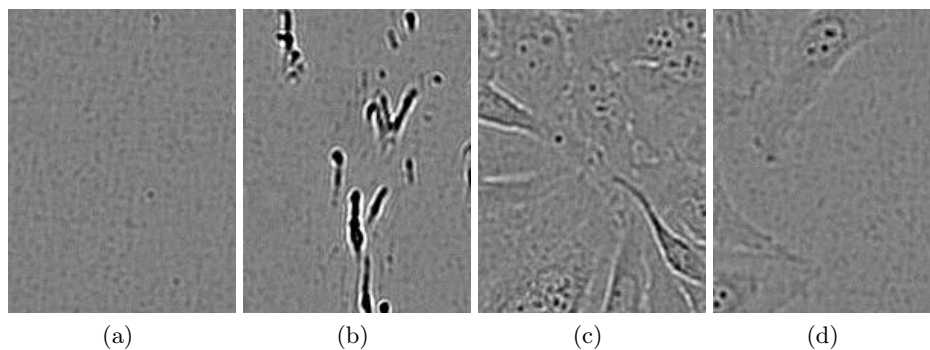


Fig. 8: Parts of the scratch array images: (a) background, (b) dirt, (c) cell area, (d) weak wound boundary.

6 Conclusion

In this manuscript, a new database for scratch assay analysis has been presented and made publicly available, together with the implementation of two wound area detection algorithms. There is little publicly available data on scratch assays, and even these datasets contain only a few images. Therefore, the introduced database contributes considerably to the available quantity. The presented database offers several advantages over the already available ones: it consists of

a sequence of 34 high-resolution raw images, each image covering the entire cell layer in a well, thus offering the possibility to study the cell migration process over the entire scratch area. Existing tools in this area are designed to assist a scratch assay expert in the task of measuring cell migration and wound healing processes, but do not necessarily support a fully automated evaluation process. This manuscript and the published algorithm should help to drive the development in this direction. Challenges encountered during the development of fully automated wound segmentation tasks are highlighted in the discussion section, along with steps for future work. In general, it could be stated that the algorithms for scratch assay assessment have the potential for improvement towards better generalization, i.e. these algorithms can be more easily applied to new data from different acquisition systems to consistently produce reliable segmentation results. As a consequence, there is great interest in applying deep learning approaches, such as convolutional neural networks (CNNs), to the problem of wound healing assessment. These approaches would also require a large amount of available data for training.

The presented results of the algorithms now published serve as an initial benchmark on the newly introduced database and thus contribute to the field of scratch assay assessments.

Acknowledgments. This research was funded by the Salzburg State Government within the Science and Innovation Strategy Salzburg 2025 (WISS 2025) under the project AIIV-Salzburg (Artificial Intelligence in Industrial Vision), project no 20102-F2100737-FPR.

Disclosure of Interests. The authors have no competing interests to declare that are relevant to the content of this article.

References

1. Carpenter, A.E., Jones, T.R., Lamprecht, M.R., Clarke, C., Kang, I.H., Friman, O., Guertin, D.A., Chang, J.H., Lindquist, R.A., Moffat, J., Golland, P., Sabatini, D.M.: CellProfiler: image analysis software for identifying and quantifying cell phenotypes. *Genome Biol* **7**(10), R100 (Oct 2006)
2. Cortesi, M., Pasini, A., Tesei, A., Giordano, E.: Aim: A computational tool for the automatic quantification of scratch wound healing assays. *Applied Sciences* **7**(12) (2017)
3. Gebäck, T., Schulz, M.M.P., Koumoutsakos, P., Detmar, M.: TScratch: a novel and simple software tool for automated analysis of monolayer wound healing assays. *Biotechniques* **46**(4), 265–274 (Apr 2009)
4. Glaß, M., Möller, B., Zirkel, A., Wächter, K., Hüttelmaier, S., Posch, S.: Scratch assay analysis with topology-preserving level sets and texture measures. In: Vitrià, J., Sanches, J.M., Hernández, M. (eds.) *Pattern Recognition and Image Analysis*. pp. 100–108. Springer Berlin Heidelberg, Berlin, Heidelberg (2011)
5. Glaß, M., Möller, B., Zirkel, A., Wächter, K., Hüttelmaier, S., Posch, S.: Cell migration analysis: Segmenting scratch assay images with level sets and support vector machines. *Pattern Recognition* **45**(9), 3154–3165 (2012), best Papers of Iberian Conference on Pattern Recognition and Image Analysis (IbPRIA’2011)

6. Grada, A., Otero-Vinas, M., Prieto-Castrillo, F., Obagi, Z., Falanga, V.: Research techniques made simple: Analysis of collective cell migration using the wound healing assay. *Journal of Investigative Dermatology* **137**(2), e11–e16 (2017)
7. Jalilian, E., Linortner, M., Uhl, A.: Impact of image compression on in-vitro cell migration analysis. *Computers* **12**(5), 98 (2023)
8. Javer, A., Rittscher, J., Sailem, H.Z.: DeepScratch: Single-cell based topological metrics of scratch wound assays. *Comput Struct Biotechnol J* **18**, 2501–2509 (Aug 2020)
9. Jonkman, J.E.N., Cathcart, J.A., Xu, F., Bartolini, M.E., Amon, J.E., Stevens, K.M., Colarusso, P.: An introduction to the wound healing assay using live-cell microscopy. *Cell Adh Migr* **8**(5), 440–451 (2014)
10. Kamensky, L., Jones, T.R., Fraser, A., Bray, M.A., Logan, D.J., Madden, K.L., Ljosa, V., Rueden, C., Eliceiri, K.W., Carpenter, A.E.: Improved structure, function and compatibility for CellProfiler: modular high-throughput image analysis software. *Bioinformatics* **27**(8), 1179–1180 (02 2011)
11. Liang, C.C., Park, A.Y., Guan, J.L.: In vitro scratch assay: a convenient and inexpensive method for analysis of cell migration in vitro. *Nature Protocols* **2**(2), 329–333 (Feb 2007)
12. Ljosa, V., Sokolnicki, K.L., Carpenter, A.E.: Annotated high-throughput microscopy image sets for validation. *Nature Methods* **9**(7), 637–637 (Jul 2012)
13. Möller, B., Posch, S.: Comparing active contours for the segmentation of biomedical images. In: 2012 9th IEEE International Symposium on Biomedical Imaging (ISBI). pp. 736–739 (2012)
14. Sinitca, A.M., Kayumov, A.R., Zelenikhin, P.V., Porfiriev, A.G., Kaplun, D.I., Bogachev, M.I.: Segmentation of patchy areas in biomedical images based on local edge density estimation. *Biomedical Signal Processing and Control* **79**, 104189 (2023)
15. Suarez-Arnedo, A., Figueroa, F.T., Clavijo, C., Arbeláez, P., Cruz, J.C., Muñoz-Camargo, C.: An ImageJ plugin for the high throughput image analysis of in vitro scratch wound healing assays. *PloS one* **15**(7) (2020)
16. Topman, G., Sharabani-Yosef, O., Gefen, A.: A standardized objective method for continuously measuring the kinematics of cultures covering a mechanically damaged site. *Medical Engineering & Physics* **34**(2), 225–232 (2012)
17. Zaritsky, A., Natan, S., Horev, J., Hecht, I., Wolf, L., Ben-Jacob, E., Tsarfaty, I.: Cell motility dynamics: A novel segmentation algorithm to quantify multi-cellular bright field microscopy images. *PLOS ONE* **6**(11), 1–10 (11 2011)